

## Optical rotation curves beyond the HI cut-off in spirals

J. Bland-Hawthorn

*Anglo-Australian Observatory, P.O. Box 296, Epping, NSW 2121, Australia*

**Abstract.** In the best observed spiral galaxies, the HI is observed to decline slowly with radius for up to 90% of the maximum extent, before experiencing a rapid truncation. Early models predicted that the outer parts of spirals would be fully ionized by a metagalactic UV field at column depths of roughly  $10^{19}$  atoms  $\text{cm}^{-2}$ . Weak optical line emission has now been observed beyond the HI edge in a number of cases and, furthermore, this warm gas has been used to trace the dark halo far beyond the HI cut-off. But the observed emission measures (40–90 mR) are higher than expected for a cosmic origin. A more likely explanation is ionization of the warped outer disk by the blue stellar population at smaller radius. There are many implications of ionized warped edges, in particular, severe HI warps may be greatly under represented in current HI surveys. We briefly discuss the implications of this model for the Galactic warp.

### 1. Introduction

Bochkarev & Sunyaev (1977) first argued that the HI disks of spiral galaxies truncate at a few times the optical diameter because the exponentially declining HI column eventually becomes fully ionized by a metagalactic UV field. After detailed calculations of the expected emission measures (Maloney 1993; Dove & Shull 1994), it was soon realized that these extremely faint levels could be reached with the Fabry-Perot ‘staring’ technique (Bland-Hawthorn *et al.* 1994; hereafter BTVS). This method has since been used successfully on Sculptor galaxies (Bland-Hawthorn, Freeman & Quinn 1997; hereafter BFQ), M33 and NGC 3198 (Bland-Hawthorn, Veilleux & Carignan 1998; hereafter BVC). In keeping with the main focus of this workshop, we start with a brief discussion of the dark halo in NGC 253. But most of the article will be devoted to the source of the HI truncation.

### 2. The dark halo of NGC 253

In Fig. 1*a–c*, we show the kinematic measurements along the major axis of NGC 253 deduced from VLA HI (inner points), TAURUS-2 H $\alpha$  and [NII] lines (outer 4 points). The HI data are from a fit to the full velocity field (Puche, Carignan & van Gorkom 1991; hereafter PCvG). Whether one fits to the approaching side, receding side, or the full velocity field, the rotation curve is still rising in

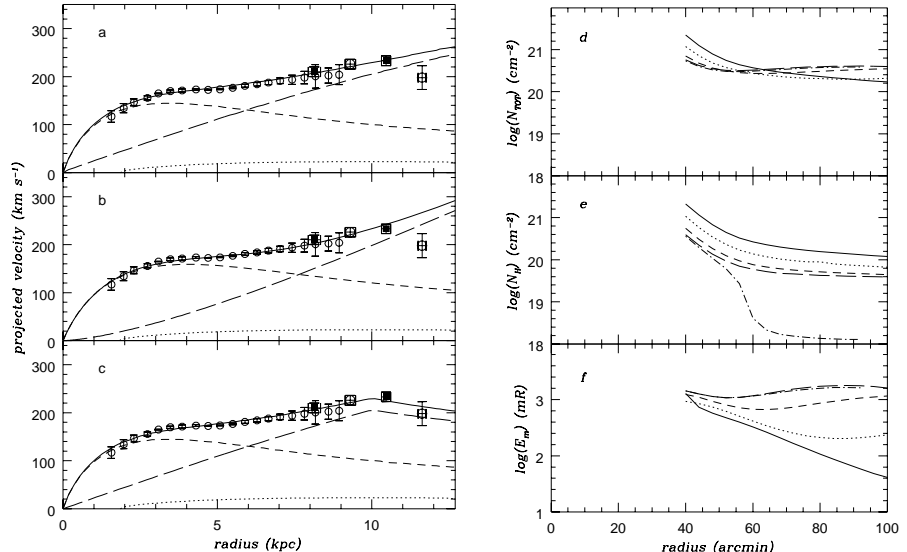


Figure 1. In the left panel ( $a - c$ ), the HI, H $\alpha$  and [NII] rotation curves are shown with representative models for NGC 253 (see text). In the right panel ( $d - f$ ), we illustrate the influence of an ionizing disk on different warp extremes in M33. We show the projected HI, seen from the galaxy nucleus, before ( $d$ ) and after ( $e$ ) the disk ionization is switched on, and the resulting trend ( $f$ ) in emission measure with radius. The deprojected HI data are from Corbelli & Schneider (1997).

the outermost parts, a phenomenon observed in a number of low mass spirals (Puche & Carignan 1991).

The inflexion in the rotation curve is understood naturally to arise from the potential of an exponential stellar disk with a much larger dark halo (*e.g.*, Carignan & Freeman 1985). To illustrate this (Fig. 1a – c), we show representative fits to the PCvG and TAURUS-2 data using a 3-component mass model (disk, halo, gas). The contribution from the HI surface density (dotted line) is the same in all models. In *a*, we adopt an exponential disk (short-dashed line) and choose an isothermal sphere for the spherical halo (long-dashed line) using the numerical approach developed by Carignan (1985). In *b*, we have used the disk-halo models of Dehnen & Binney (1997). In *c*, we have truncated the halo at a radius of 10 kpc to demonstrate a possible explanation for the last measured point. (A detailed discussion is given in BFQ.)

The outermost TAURUS-2 H $\alpha$  measurement suggests that the rotation curve may be falling beyond a radius of about 10 kpc, but there are certainly other possible explanations for its low observed velocity (*e.g.*, tidal forces). But BFQ consider the possibility that the rotation curve of NGC 253 is indeed falling beyond 10 kpc due to a truncated dark halo (see Fig. 1c). This compares to the much larger dark halo distributions observed in our Galaxy (*e.g.*, Freeman 1996) and other large spirals (*e.g.*, Zaritsky *et al.* 1996).

If this interpretation is correct, there are some interesting consequences. The properties of dark halos are best studied in disk galaxies for which the HI distribution extends well beyond the optical distribution. In the outer regions

of these galaxies, the ratio of (dark matter surface density)/(HI surface density) is roughly constant (*e.g.*, Bosma 1978; Carignan 1991). NGC 253 is not such a galaxy. Its HI extends only 40% further than the optical extent. But the data provide the first hint that where the HI and the light are co-extensive, the dark matter also may not extend much beyond the optical distribution. It is tentative evidence of the apparent link between the dark matter and the HI. We emphasize that the dark matter is still essential to generate the observed rotation curve for NGC 253: the inferred mass ratio of dark matter to luminous matter is about 5.

### 3. What ionizes the outer edge of NGC 253?

In NGC 253, we see ionized gas with  $\mathcal{E}_m \approx 40\text{--}90$  mR at and beyond the HI edge. The [NII] $\lambda 6548$ /H $\alpha$  ratio is close to unity which is anomalously high for diffuse gas.

**Young stellar disk.** BFQ attempt to explain this enhancement with recourse to standard ionization codes and an idealised model for the young disk (see Bland-Hawthorn & Maloney 1997; 1998; hereafter BM). A useful approximation to this model, and the predicted halo fluxes, are given in the appendix. Since essentially all spirals are warped, it is likely that this interpretation has application to a large fraction of objects. P.R. Maloney has calculated the HI truncation produced by our model in the context of M33 (Fig. 1d – f). The curves correspond to integral sign warps with a range of maximum amplitudes: 10° (solid), 20° (dot), 40° (short dash), 60° (long dash), modified 60° (dot-dash). The last curve is the same as the previous curve except that the column density has been reduced by 5%. The existence of a truncated edge is very sensitive to the ionizing flux and the shape of the warp.

An important prediction of the models is that most of the low ionization lines are greatly enhanced with respect to H $\alpha$ , and that [OIII]5007 is essentially invisible. This has largely been confirmed from a run in October 1997 with K.C. Freeman at the MSO 2.3m using the Double Beam Spectrograph. We obtained a total exposure time of 5.6 hours at field positions SW3 and SW4 (BFQ). The stacked data reveal that, like [NII]/H $\alpha$ , [SII]/H $\alpha$  is extraordinarily high ( $\approx 0.5 - 0.8$ ) in agreement with the model.

**Cosmic ionizing background.** From H $\alpha$  non-detections towards extragalactic HI, the current best  $2\sigma$  upper limit (Vogel *et al.* 1995) for the cosmic ionizing background is  $J_{-21}^o < 0.08$  ( $\Phi^o < 2\text{--}4 \times 10^4$  phot cm $^{-2}$  s $^{-1}$ ; see appendix). This compares with  $J_{-21}^o \approx 0.006$  deduced from the proximity effect (Kulkarni & Fall 1995). If the 3C 273 sight line is truly representative, the Milky Way dominates the ionizing field out to 400 kpc on average, and maybe 700 kpc along the polar axis. This is an order of magnitude smaller than the scale of typical  $L_*$  galaxy separations at the present epoch.

BTVS show that the expected emission measure from a cloud is unlikely to be detectable beyond 300 kpc, or maybe 500 kpc along the polar axis. This has a number of important ramifications, *e.g.*, it is unlikely we can detect the mutual ionization of M31 and the Galaxy. At this meeting, L. Blitz has laid claim to a large fraction of high velocity clouds, placing them at extragalactic distances

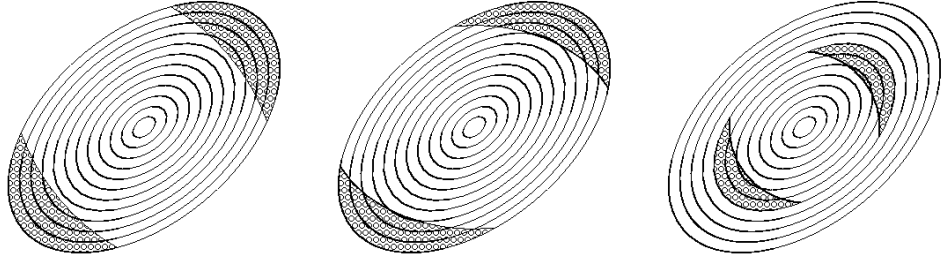


Figure 2. Ionized outer regions arising from (a) a simple warp, (b) a precessing warp, and (c) a simple warp that folds back on itself.

within the Local Group. However, if most of these clouds produce detectable  $H\alpha$ , this interpretation is unlikely to be correct.

**Suprathermal particle heating.** The enhanced low ionization lines require substantial heating of the gas without further ionization. BFQ go some way to achieving this with a dilute, hardened radiation field impinging on gas with refractory element depletion. But the required heating rate is too low by at least a factor of two. Many early candidates (*e.g.*, relativistic particles) have proved unsuccessful. More promising are subrelativistic, heavy (suprathermal) particles channelled along magnetic field lines to the outer disk. Their stopping lengths can be very long so that the ionization rate is kept low, and a single nucleus can produce many energetic “knock on” electrons.

#### 4. HI disk morphology

There are a number of interesting consequences arising from global ionization of the outer disk. Here, we illustrate how different sources could produce quite distinct behaviour in (i) the outer HI disk morphology, and (ii) the trend in  $\mathcal{E}_m$  with radius. In the next section, we consider the special case of the Galactic warp.

In the table below, the deprojected shape of the HI disk at a fixed column density is shown in the first column. The source of the truncation and the expected trend in  $\mathcal{E}_m$  (with increasing radius) are given in the second and third columns respectively:

<i>shape of HI disk</i>	<i>source of truncation</i>	<i>radial trend</i>
mirror symmetric	integral-sign warp + internal source	$\mathcal{E}_m$ increasing
axisymmetric	ambient radiation field	$\mathcal{E}_m$ decreasing
bisymmetric	tides due to external galaxy	$\mathcal{E}_m = 0$
asymmetric	ram pressure from external medium	$\mathcal{E}_m$ complex

The first interpretation assumes a simple warp for the HI, a characteristic of most warps (Briggs 1990), although one can certainly construct different scenarios (see Fig. 2) for ionization by a central source. The prediction of  $\mathcal{E}_m$  increasing is confirmed in Fig. 1*f* although only in the limit of strong warps ( $> 30^\circ$ ). These models predict azimuthal incompleteness in the HI distribution at critical velocities. Careful kinematic analysis of the best observed spirals could put strong limits on each of these models. The second interpretation is the conventional picture in terms of a metagalactic UV field (see §1) but, to date, we see no evidence for such a model. The third and fourth models are speculative at best: it is difficult to see how either could produce well defined HI truncations.

In order to explore these different cases, we are currently studying a range of galaxy types in different environments, with the aim of tracing the dark matter beyond the HI limit. The galaxies chosen for detailed study include M31, M33, M81, M83, NGC 628, NGC 3198, NGC 5266, Fourcade-Figueroa, and the Sculptor Group. The most detailed work has concentrated on NGC 253 (BFQ), M33 and NGC 3198 (BVC).

## 5. The Galaxy

In Fig. 3, we illustrate the predicted halo ionizing field. The 21 cm data are from Burton (1984) and Burton & de Lintel Hekkert (1986). This is normalized to explain the Magellanic H $\alpha$  stream detections (Weiner & Williams 1996). The northern HI warp is easily truncated by the disk radiation; we suggest that the southern warp is much less pronounced due to the ionizing influence of both the LMC and the inner disk.

The predicted levels of H $\alpha$  emission should be easily detectable (150–200 mR) with WHAM, and only marginally by other all-sky H $\alpha$  surveys. We anticipate that the projected H $\alpha$  emission off the plane will show peaks at  $l = 70^\circ$  and  $l = 250^\circ$  respectively, with the southern extension being more pronounced. It should be possible to extend the Galactic rotation curve beyond the current HI limit. More generally, it seems highly likely that severe warps in spirals, particularly those with UV-bright inner disks, are suppressed by disk ionization.

## 6. Discussion

The ionization models for warped edges suggest that essentially any spiral with a young, stellar population can be reasonably traced to and beyond the HI limit. In the months to come, there will be half a dozen spirals with optical rotation curves at and beyond the HI edge. For these objects, the total mass in H $^+$  is comparable to the HI mass.

It is possible to use the ‘staring’ method down to surface brightness levels at least 6 magnitudes below sky in a 1Å band (BTVS). It may be possible to extend this limit further with telescope nodding, charge shuffling and deep depletion CCD arrays, all of which will be in place at the AAT by early 1998. *In principle*, stellar rotation curves can be traced to several magnitudes below sky, although the Lorentzian instrumental profile is a handicap to reaching much beyond a Holmberg radius! There are good reasons for pushing the stellar rotation curves.

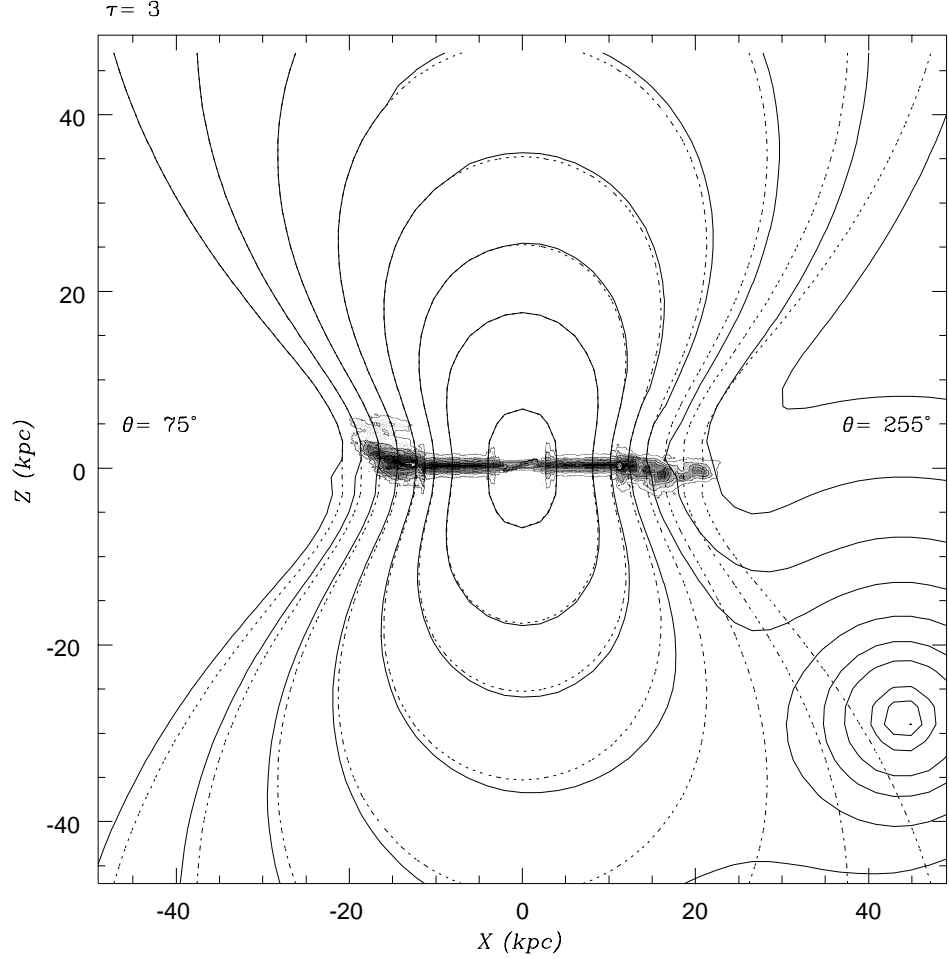


Figure 3. The galactic halo ionizing field. The coordinates are with respect to a plane perpendicular to the Galactic disk (with the Galactic Centre at the origin) at a constant galactic azimuth angle ( $75^\circ$ ,  $255^\circ$ ). The dotted lines show the ionizing flux ( $\varphi_4$ ) due to the galactic disk; the solid lines include the contribution from the LMC. The opacity of the HI disk (shown in half tone) has been included. The contours, from outside in, are for  $\log \varphi_4 = 1, 1.25, 1.5, 1.75, 2, 2.25, 2.5, 3$  phot  $\text{cm}^{-2} \text{s}^{-1}$ . The minor contribution from the Galactic corona is omitted (BM).

In special cases, the  $H^+$  kinematics may need second order corrections (*e.g.*, asymmetric drift) for ionization effects (*e.g.*, Yorke, Bodenheimer & Tenorio-Tagle 1982; Yorke & Welz 1996).

We stress that 21 cm mapping of spirals is crucial to this work, and is substantially more efficient than ‘staring’ over the HI extent. (For reasons outlined in §4, it is even worth the effort to revisit archived 21 cm data.) It takes 0.5–1 nights to obtain a pair or triplet of optical kinematic measurements. More rapid progress is possible with a dedicated 2.5m–5m telescope (see BFQ, eqn. 7). These measurements are tied to the HI data and must be corrected for warping (and flaring) of the disk. While Fabry-Perot ‘staring’ has extraordinary potential for many problems, *e.g.*, R.J. Reynolds’ outstanding work with the WHAM instrument, it merely complements the deepest measurements obtainable in other bands.

**Acknowledgments.** I am indebted to K.C. Freeman, P.R. Maloney, H.W. Yorke, W.B. Burton, and M.A. Dopita for assistance with several aspects of this work.

## References

- Bland-Hawthorn, J., Taylor, K., Veilleux, S. & Shopbell, P.L. 1994, ApJ, 437, L95
- Bland-Hawthorn, J., Freeman, K.C. & Quinn, P.J. 1997, ApJ, 490, 143
- Bland-Hawthorn, J. & Maloney, P.R. 1997, PASA, 14, 59
- Bland-Hawthorn, J. & Maloney, P.R. 1998, ApJ, submitted
- Bland-Hawthorn, J., Veilleux, S. & Carignan, C. 1998, ApJ, in preparation
- Bochkarev, N.G. & Sunyaev, R.A. 1977, Soviet Astr., 21, 542 (originally 1975, AZh, 54, 957)
- Bosma, A. 1978, PhD, University of Groningen
- Briggs, F. 1990, ApJ, 352, 15
- Burton, W.B. 1984, in Galactic & Extragalactic Radio Astronomy, eds. K.I. Kellerman and G.L. Verschuur (Springer-Verlag), p. 82
- Burton, W.B. & te Lintel Hekkert, P. 1986, A&AS, 65, 427
- Carignan, C. 1985, ApJ, 299, 59
- Carignan, C. 1991, contribution to Space Telescope Workshop on Dark Matter.
- Carignan, C. & Freeman, K.C. 1985, ApJ, 294, 494
- Corbelli, E. & Schneider, S.E. 1997, ApJ, 479, 244
- Dehnen, W. & Binney, J. 1997, MNRAS, 287, 5
- Dove, J.B. & Shull, J.M. 1994, ApJ, 423, 196
- Freeman, K.C. 1996, in Unsolved Problems of the Milky Way, ed L. Blitz and P. Teuben (Dordrecht: Kluwer), p. 645.
- Kulkarni, V.P. & Fall, M. 1995, ApJ, 453, 65
- Maloney, P.R. 1993, ApJ, 414, 41
- Puche, D. & Carignan, C. 1991, ApJ, 378, 487
- Puche, D., Carignan, C. & van Gorkom, J. 1991, AJ, 101, 456

- Vogel, S.N., Weymann, R., Rauch, M. & Hamilton, T. 1995, ApJ, 441, 162  
 Weiner, B.J. & Williams, T.B. 1996, AJ, 111, 1156  
 Yorke, H., Bodenheimer, P. & Tenorio-Tagle, G. 1982, A&A, 108, 25  
 Yorke, H. & Welz, A. 1996, A&A, 315, 555  
 Zaritsky, D., Smith, R., Frenk, C., & White, S. 1996, ApJ, 478, 39

## A Ionization models

We present a useful approximation to the Galactic halo ionizing field deduced by BM. We assume an electron temperature  $T_e \simeq 10^4\text{K}$ , as expected for gas photoionized by stellar sources, for which the Case B hydrogen recombination coefficient is  $\alpha_B \simeq 2.6 \times 10^{-13} (10^4/T_e)^{0.75} \text{ cm}^3 \text{ s}^{-1}$ . At these temperatures, collisional ionization processes are negligible. In this case, the column recombination rate in equilibrium must equal the normally incident ionizing photon flux,  $\alpha_B n_e N_{H^+} = \varphi_i$ , where  $\varphi_i$  is the rate at which LyC photons arrive at the cloud surface (photons  $\text{cm}^{-2} \text{ s}^{-1}$ ),  $n_e$  is the electron density and  $N_{H^+}$  is the column density of ionized hydrogen. The emission measure is  $\mathcal{E}_m = \int n_e n_{H^+} dl = n_e n_{H^+} L \text{ cm}^{-6} \text{ pc}$  where  $L$  is the thickness of the ionized region. The resulting emission measure for an ionizing flux  $\varphi_i$  is then  $\mathcal{E}_m = 1.25 \times 10^{-2} \varphi_4 \text{ cm}^{-6} \text{ pc}$  ( $= 4.5 \varphi_4 \text{ mR}$ ) where  $\varphi_i = 10^4 \varphi_4$ . For an optically thin cloud in an isotropic radiation field, the solid angle from which radiation is received is  $\Omega = 4\pi$ , while for one-sided illumination,  $\Omega = 2\pi$ . For our disk model, however,  $J_\nu$  is anisotropic and  $\Omega$  can be considerably less than  $2\pi$ .

For the cosmic field,  $J_{-21}^o$  is the ionizing flux density of the cosmic background at the Lyman limit in units of  $10^{-21} \text{ erg cm}^{-2} \text{ s}^{-1} \text{ Hz}^{-1} \text{ sr}^{-1}$ ;  $\Phi^o$  ( $= \pi J_{-21}^o/h$ ) is the equivalent photon flux at face of a uniform, optically thick slab.

For the Galactic halo (Fig. 3), to a good approximation, the poloidal UV radiation field is

$$\varphi_4 = 2.8 \times 10^6 e^{-\tau} r_{\text{kpc}}^{-2} \cos^{0.6\tau+0.5} \Theta \quad \text{phot cm}^{-2} \text{ s}^{-1} \quad (1)$$

where  $\Theta$  is the polar angle ( $0 \leq \Theta < \frac{\pi}{2}$ ) and the Lyman limit optical depth  $\tau \leq 10$ . It follows that the solid-angle averaged flux is

$$\bar{\varphi}_4 = \frac{2.8 \times 10^6 e^{-\tau}}{(0.6\tau + 1.5)r_{\text{kpc}}^2} \quad \text{phot cm}^{-2} \text{ s}^{-1}. \quad (2)$$

In order to explain Magellanic Stream  $\text{H}\alpha$  detections, our model favours  $\tau \approx 2.8$ .